AN INVESTIGATION OF REGIONAL DEPENDENCE OF THE SLOPE OF THE INITIAL PART OF P-WAVE ENVELOPE

Lian Chao[*] **Supervisor: Tatsuhiko HARA** **
MEE12602

ABSTRACT

We investigated regional dependence of the slope of the initial part of P-wave envelope, which is used to determine epicentral distances in the Japan Meteorological Agency and Japan Railway Company earthquake early warning (EEW) systems. The Tohoku region was chosen as the study region. We retrieved 19,899 strong motion borehole data for 265 events with magnitudes in the range from 5.0 to 7.6 from KiK-net (Kiban Kyoshin network). Following previous studies, we fitted the function $Bt \cdot \exp(-At)$ to the initial part of P-wave envelopes to obtain sets of the parameters of *A* and *B* and obtained the following relation $\log B = -2.27 \cdot \log \Delta + 4.07$ by the least squares method. This is consistent with the previous study which used the data set similar to that of this study within one standard deviation. Then, we determined intercepts of the above formula for each event keeping the slope to -2.27 to investigate the regional dependence. There appear two tendencies; shallow crust events have lower values of c, and deeper events in the subducting slab have higher values of *c*. We examined the *B* values obtained for the same set of the stations for the selected three events, and found that their differences are significant. These results suggest that the differences of the coefficient c are likely to be due to earthquake characteristics.

Keywords: EEW, *B*-Δ method, regional dependence.

1. INTRODUCTION

When large earthquakes occur, Earthquake Early Warning (EEW) can alert areas near the epicenter for imminent strong ground shaking. There are two kinds of approach in EEW, the onsite approach and the regional approach. The onsite approach uses the P-wave at the site to estimate ground motion at the same site. The Pd approach (Wu and Kanamori, 2005) and threshold-based approach (Colombelli *et al*., 2012) are examples of this approach. The regional approach estimates magnitude and location by using data from seismic stations. UrEDAS (Nakamura, 1988), Elarms (Allen and Kanamori, 2003), Tau_c (Kanamori, 2005), and SAS (Igresias *et al*., 2007) belong to the regional approaches category. The Japan Meteorological Agency (JMA) adopted the regional approach, and implemented its emergency earthquake alarm system. It provided the early warning information as experimental data for universities and other organizations on 25 February 2004 and has started issuing the earthquake warning for public from 1 October 2007. The basic methodology is described in Kamagaichi (2004) and Kamigaichi *et al*. (2009).

2. *B*-Δ METHOD

[*]Earthquake Administration of Hubei Province, CEA.
[**]International Institute of Seismology and Earthquake Engineering, Building Research Institute (IISEE, BRI), Tsukuba, Japan.

Odaka *et al*. (2003) fitted the following function to the initial part of the P-wave envelope:

$$f = Bt \cdot \exp(-At) \tag{1}$$

where A and B are unknown parameters, t is the time from P-wave arrival. They evaluated the parameters A and B for several earthquakes showing that log B is linearly proportional to –log Δ, and the relation between log B and log Δ did not significantly depend on earthquake magnitude. Therefore, they suggested that the epicentral distance could be estimated immediately after the P-wave arrival by using this relation. Tsukada *et al*. (2004) obtained this relation between B and Δ by their further analyses. This method is called the *B*-Δ method, and is used as a single station method to determine epicentral distance in JMA and Japan Railway Company EEW systems. Nakamura *et al*. (2007) suggested the possible regional dependence of the coefficient B.

3. DATA RANGE

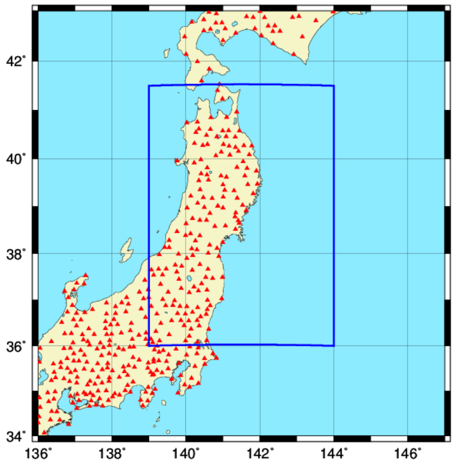

Figure 1. The study area (the blue rectangle) and KiK-net stations (the red triangles) in and around the study area.

We used strong motion data from KiK-net (Kiban kyoshin network, Aoi *et al*., 2000) in this study to which the *B*-Δ method was applied. KiK-net is a strong motion network deployed by the National Research Institute for Earth Science and Disaster Prevention (NIED). The format of KiK-net data follows that of the K-NET (Kyoshin network, Kinoshita, 1998). We chose the Tohoku area as the study region. Figure 1 shows the study area and the KiK-net stations in and around it. 265 events were selected in order to obtain 19,899 strong motion data, to which the B-Δ method was subsequently applied. The magnitude range, period and region of the events are shown in Table 1. Most of the events after the 2011 off the Pacific coast of Tohoku Earthquake occurred in the sea area.

Table 1. The magnitude range, period and region of the events (4 March 2007 – 25 April 2007).

Magnitude	Period	Region	Numbers of events
>=7	2011.1.1~2013.5.30	E139~144, N36~41.5	6
	1997.1.1~2010.12.30		2
6.0~6.9	2011.1.1~2013.5.30	E139~144, N36~41.5	44
	1997.1.1~2010.12.30		22
5.0~5.9	2011.1.1~2013.5.30	E139~144, N36~41.5	173
	1997.1.1~2010.12.30	E139~142, N36~41.5	18

4. DATA ANALYSIS PROCEDURE

In order to decrease the effect of shallow structures on seismic records, vertical component borehole data (UD1) were used for the application of the *B*-Δ method to investigate regional dependence. First, KiK-net data were retrieved in the K-NET ASCII format, and then converted to the SAC binary format.

Second, automatic pickings were done as follows. The application of band-pass filter and squaring of each data point had been done, and then STA (short time average) and LTA (long time average) rates have been used to determine P-wave arrival. A band-pass filter with corner frequencies between 5 and 10 Hz was adopted. The STA window was set to 0.05s and LTA window to 1s. The threshold of the STA/LTA rate was set to 25. If the rate was more than 25 it was considered a P-wave arrival time. We found that the signals with lower frequency contents often arrived earlier than the times determined by the automatic picking. In order to get accurate results, visual confirmation and manual picking are performed for all of the data.

Third, we applied the *B*-Δ method to the prepared data. The time window for the analysis was set to 2 sec. An example of the application of the *B*-Δ method is shown in Figure 2.

The earthquake occurred on 18 June 2012, with position of N38.87, E142.09. The depth of this event was 46.8km and the magnitude of 6.1 was determined by the JMA. The solid black curve in Figure 2 shows the time series obtained by taking absolute values of the waveform data. The red curve in Figure 2 is the envelope. The least squares method is used to determine the coefficients *A* and *B* of Eq. (1) using logarithmic waveforms of this envelope as data following Odaka *et al*. (2003). The blue curve in Figure 2 is the fitted curve obtained by this procedure.

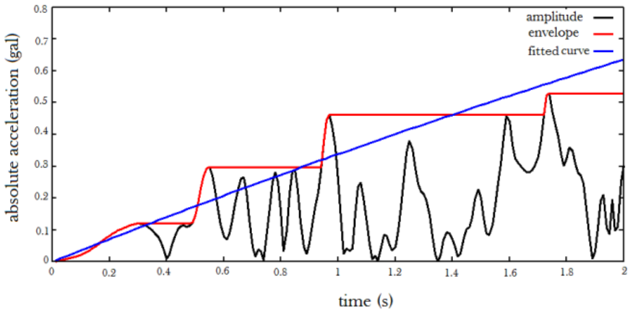

Figure 2. An example of envelope and fitted line.

5. RESULTS AND DISCUSSION

5.1. Relation between *B* and Δ

As Odaka *et al*. (2003) and Tsukada *et al*. (2004) have shown, there exists a good correlation between log *B* and log Δ. Their relation can be expressed as follows.

$$\log B = a \cdot \log \Delta + c \qquad (2)$$

where *a* and *c* are the unknown parameters to be determined by the observed log *B* and log Δ.

These coefficients were estimated using our data set. Figure 3 shows the estimated coefficients *B* and the calculated averages of log *B* for bins with widths of 0.1 for log Δ with their standard deviations. We found that the log *B* could be fitted as a straight line as a function of log Δ approximately in the range from 1.6 to 2.4. This range corresponds to the epicentral distance range from about 40 to 250 km. Therefore, data in the epicentral distance range from 40 to 250 km were chosen to calculate the coefficients *a* and *c*. Consequently, the following relation between *B* and Δ was obtained:

$$\log B = -2.27 \cdot \log \Delta + 4.07 \qquad (3)$$

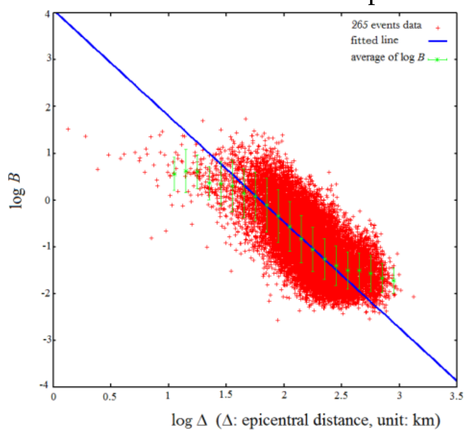

Figure 3. Relation between *B*-Δ, fitted line with coefficients *a* and *c* and errors in log *B* average.

The fitted line (the blue line in Figure 3) is close to the averages of log *B* in the log Δ range from 1.6 to 2.4.

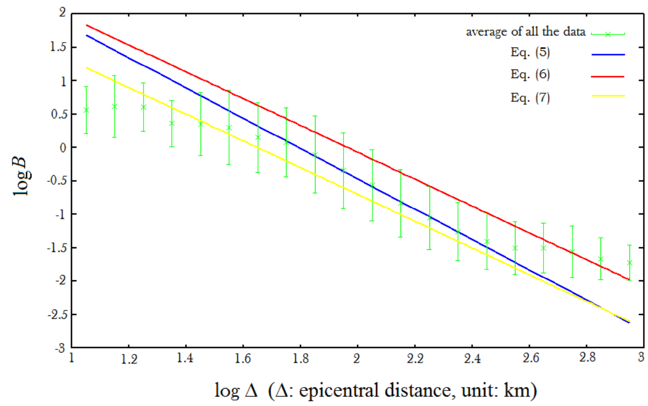

Figure 4. Comparison of relation between *B*-Δ for 265 events (Eq.(3), blue line), in JMA EEW System (Eq.(4), red line), and produced by Nakamura (Eq.(5), yellow line).

We compared our result to other formulas. Eq. (4) shows the current formula for the relation between *B* and Δ adopted by JMA, and Eq. (5) is the formula obtained by Nakamura using KiK-net data (http://www.seisvol.kishou.go.jp/eq/EEW/Meeting_HYOUKA/t03/shiryou2.pdf)

$$\log\Delta = -0.498\cdot\log B + 1.965 \quad (4)$$

$$\log\Delta = -0.5\cdot\log B + 1.65 \quad (5)$$

Figure 4 shows a comparison of the formula obtained in this study with the two formulas given above. The log *B* from Eq. (4) is systematically larger than that from Eq. (5). The log *B* (and the fitted line) of this study is closer to Eq. (5) in the larger log Δ (~2.4), while they are a little larger in the smaller log Δ (~1.6), although the differences are within the one standard deviations.

5.2. Regional dependence of coefficient *c*

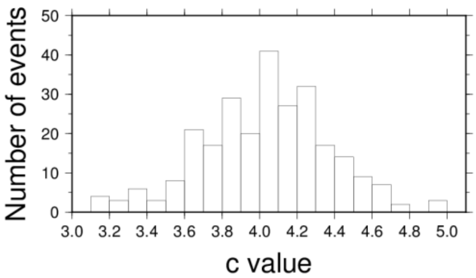

Figure 5. Histogram of coefficients *c*.

In order to study regional dependence of the coefficients of the *B*-Δ method, following Nakamura *et al.* (2007), the value of *a* in Eq.(4) was set to -2.27, and determined the coefficient *c* for each event. Figure 5 is a histogram of estimated coefficients *c*. The estimated coefficients *c* scattered around 4.0, in the range from 3.1 to 5.0.

In order to determine spatial distributions of the coefficients *c*, they were classified into three groups in the ranges of [3.1, 3.6), [3.6, 4.5) and [4.5, 5.0], respectively. Figure 6 shows the spatial distributions of these groups with their depth profiles.

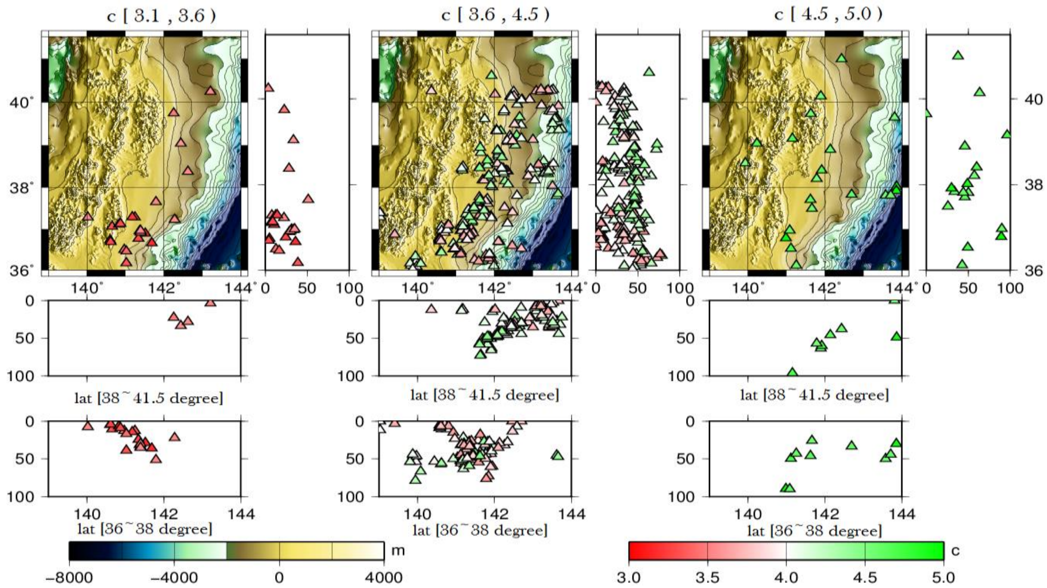

Figure 6. Distribution of coefficients *c* and depth projections of three groups; coefficient *c*: [3.0, 3.85), [3.85, 4.25) and [4.25, 5.0] and two respective longitude-depth projection graphs

The spatial distribution of events with smaller *c* values (especially in the bottom left panel of Figure 6) is different from that of events with larger *c* values (especially in the bottom right panel of Figure 6). There appears to be the following two tendencies; shallow crust events have lower values of *c*, and that deeper events in the subducting slab have higher values of *c*. The result of this study is partly consistent with Nakamura *et al.* (2007), who suggested the differences of the coefficient *c* between inland earthquakes and subduction zone earthquakes.

5.3 Examples of events with the different *c* values

Table 2. Earthquake information, *c* values for selected earthquakes (the coefficient *a* is set to -2.27)

No.	Original time	Lat (degree)	Lon (degree)	Depth (km)	M_{JMA}	*c* (*a* = -2.27)
1	2011-09-23	36.69	140.62	4.2	5.1	3.29
2	2012-06-28	37.17	141.20	63.2	5.2	4.09
3	2005-01-01	36.78	140.98	89.4	5.0	5.04

As shown above, it seems that there is a regional difference for the coefficient *c*. In order to investigate whether this difference is clear in observed *B* estimates, three events with different *c* values were selected. The magnitudes of the selected three events were 5.0, 5.1 and 5.2. The difference of the magnitude is small. Figure 7 and Table 2 show the locations and values of the coefficient *c* for these three events.

In order to reduce the possible effect of station sites, we selected the *B* estimates obtained by 28 stations which recorded all three events in the epicentral distance range from 40 to 250km, and used to determine the coefficients *c* in Eq. (4)

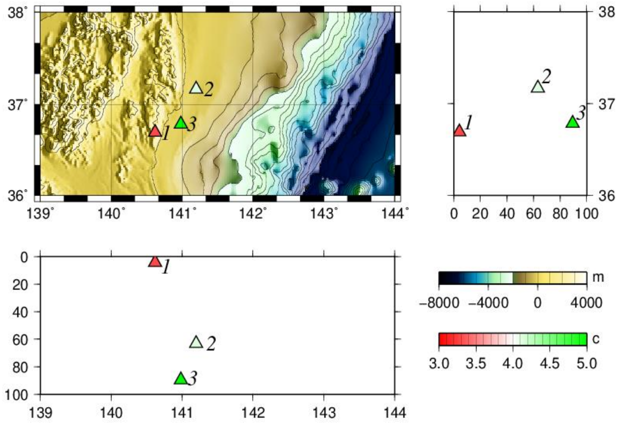

Figure 7. Three events are plotted as triangles with numbers 1, 2 and 3 listed in Table 3.

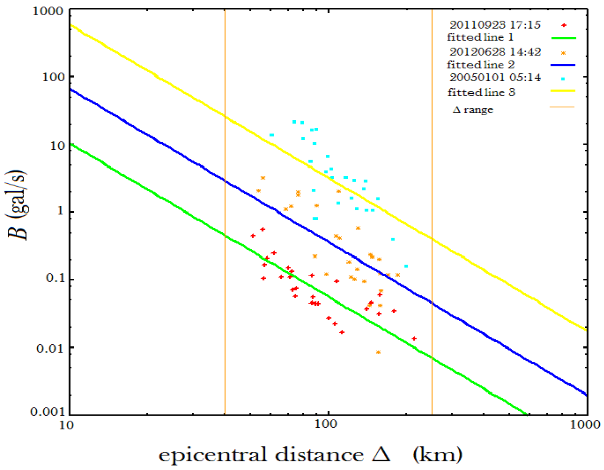

Figure 8. Relation between *B*-Δ and fitted lines for three events.

Figure 8 shows that the *B* estimates for each event are clearly different from those for other events. Event 1 that occurred in shallow crust has smaller *B* values (and smaller *c*), which results from the gentle slopes of the initial parts of P-wave envelopes, while Event 3 that occurred in subducting slab has large *B* values (and larger *c*), which results from the steep slopes. The differences shown in Figure 8 (and Figure 6) are likely to be due to earthquake characteristics, because for deeper events in the subducting slabs the structural effects such as Q (intrinsic attenuation) and scattering to affect slopes of initial P-waves are likely to be larger than or comparable to those for shallow crust events.

6. CONCLUSIONS

We investigated the relation between B and Δ and the possibility of regional dependence using earthquakes that occurred in the Tohoku region. We retrieved strong ground motion from KiK-net for 265 events and obtained 19,899 borehole data (only vertical component data were used). After automatic P-wave picking and manual confirmation, the dataset for application of the B-Δ method was prepared.

Using these dataset, we fitted the coefficients A and B for each pair of stations and events. Then, we calculated averages of log B for bins with widths of 0.1 for log Δ, and then chose the range corresponds to the epicentral distance range from about 40 to 250 km to calculate the coefficients a and c in the formula $\log B = a \log \Delta + c$ for all data. We obtained -2.27 and 4.07 for the coefficients a and c, respectively. This fitted line is close to Nakamura's result, which used a dataset similar to that of this study, for larger log Δ (~2.4), while the values of B are a little larger for smaller log Δ (~1.6), although the differences are within the one standard deviations.

By setting the slope a to -2.27, the coefficient c was re-determined separately for each event. There appears to be the following two tendencies; shallow crust events have lower values of c, and that deeper events in the subducting slab have higher values of c. From the comparison of the selected three events, the B estimates for each event are clearly different from those for other events. The differences are likely to be due to earthquake characteristics.

We are going to investigate the applicability of this method to waveform data in China following the data processing and analysis procedure in this study to contribute to development of EEW systems in China.

ACKNOWLEDGEMENTS

In this study, we used strong motion data from KiK-net (Kiban Kyoshin network) operated by the National Research Institute for Earth Science and Disaster Prevention (NIED). We also used earthquake information in "The Seismological and Volcanological Bulletin of Japan" issued by the Japan Meteorological Agency (JMA). I am grateful to Dr. Shunroku Yamamoto for his variable lecture and to Dr. Mitsuyuki Hoshiba and Dr. Hayashimoto Naoki for providing me with variable information on JMA earthquake early warning system and their comments on this work. I am grateful to Dr. Toshiaki Yokoi and Dr. Nobuo Hurukawa for their valuable advises and comments.

REFERENCES

Aoi, S. *et al.*, 2004, Journal of Japan Association for Earthquake Engineering, 4, 65-74.
Allen, R.M., and Kanamori, H., 2003, Science, 300, 685-848.
Colombelli, S. *et al.*, 2012, Bull. Seism. Soc. Am., 102, 1266-1275.
Igresias, A., Singh, S.K., Ordaz, M., 2007, Bull. Seism. Soc. Am., 97, 1718-1729.
Kamigaichi, O., 2004, J. of Japan Association for Earthquake Engineering, 4, 134-137.
Kamigaichi, O., *et al.*, 2005, Annu. Rev. Earth Planet Sci., 33,195-214.
Kinoshita, S., 1998, Seism. Res. Lett., 69, 309-332.
Kanamori, H., 2005, Annu. Rev. Earth Planet Sci., 33,195-214.
Nakamura Y., 1988, 2-9 August 1988, Japan, Railway Technical Research Institute, 7, 673-678.
Nakamura, H., *et al.*, 2007, Seism. Soc. Japan, Fall meeting, A22-09 (in Japanese).
Odaka, T., *et al.*, 2003, Bull. Seism. Soc. Am., 93, 526–532.
Tsukada, S. *et al.*, 2004, Zixin 2, 56, 351-361.
Wu, Y.M. and Kanamori, H., 2005, Bull. Seism. Soc. Am., 95, 1181–1185, doi: 10.1785/ 0120040193.